AJNR

Acquired spinal subarachnoid cysts: evaluation with MR, CT myelography, and intraoperative sonography.

E Sklar, R M Quencer, B A Green, B M Montalvo and M J Post

AJNR Am J Neuroradiol 1989, 10 (5) 1097-1104
http://www.ajnr.org/content/10/5/1097

Acquired Spinal Subarachnoid Cysts: Evaluation with MR, CT Myelography, and Intraoperative Sonography

Evelyn Sklar[1]
Robert M. Quencer[1,2]
Barth A. Green[2]
Berta M. Montalvo[1]
M. Judith Donovan Post[1]

Fifteen patients with acquired spinal subarachnoid cysts (14 surgically proved, one presumed) were evaluated preoperatively with immediate and/or delayed CT myelography (seven patients), MR (11 patients), or both (three patients). CT myelography separated subarachnoid cyst from myelomalacia and/or intramedullary cysts in four cases but failed to diagnose them in three, while MR accurately diagnosed subarachnoid cyst in all 10 cases that were also surgically proved. The results of these preoperative examinations were evaluated to determine the efficacy of each study in diagnosing subarachnoid cysts, ascertaining their extent and internal architecture, and detecting associated abnormalities of the spinal cord. In addition, during surgery these cysts were studied with sonography to gain an understanding of the pathophysiological mechanisms involved in their formation and propagation and to guide the surgeon in their decompression.

On the basis of our experience, MR appears to be the most efficient preoperative study in diagnosing and characterizing acquired subarachnoid cyst and associated abnormalities. Intraoperative sonography provides a reliable means of ensuring adequate decompression of these cysts.

***AJNR* 10:1097–1104, September/October 1989; *AJR* 153: November 1989**

Extramedullary intraspinal CSF-containing cysts can occur as primary lesions, termed arachnoid cysts, or as the sequelae of chronic inflammation or trauma [1, 2], in which case the term subarachnoid cyst (SAC) is used. The definitive radiologic diagnosis of spinal SAC is difficult. In the past, radiographic evaluation has included plain films, Pantopaque myelography, and most recently water-soluble myelography followed by CT [3–5]. Plain films reveal primarily associated bony abnormalities, while myelography may be nondiagnostic if the cysts do not fill with contrast—and in those cases it may be impossible to differentiate them from noncystic space-occupying lesions [2, 6]. In addition, if a block is present, a diagnosis is frequently not possible.

Since the radiologic diagnosis of SAC in the past has been difficult, we undertook our study to see if the new methods were more helpful. In this article we report the use of MR imaging in 11 patients and the use of CT myelography in seven patients who had acquired SAC. Of 14 patients who underwent surgery, 12 were evaluated with intraoperative spinal sonography (IOSS). It is our objective to compare the results of MR imaging with those of CT myelography to determine which is the most accurate method for evaluating patients suspected of having SAC and to demonstrate the role of IOSS in the surgical management of these patients.

Materials and Methods

A retrospective analysis of the imaging studies in 15 patients with acquired SAC was undertaken. Eleven patients were evaluated with MR imaging, seven with CT myelography

Received November 17, 1988; revision requested December 28, 1988; revision received January 25, 1989; accepted February 8, 1989.

Presented in part at the annual meeting of the Roentgen Ray Society, Miami Beach, April 1987.

[1] Department of Radiology, University of Miami School of Medicine/Jackson Memorial Medical Center, P.O. Box 016960, Miami, FL 33101. Address reprint requests to E. Sklar.

[2] Department of Neurological Surgery, University of Miami School of Medicine, Miami, FL 33101.

0195-6108/89/1005–1097

TABLE 1: Clinical Data and Imaging Results in Acquired Spinal Subarachnoid Cysts

Case No.	Age at Injury	Time from Injury to Present Evaluation	New Symptoms	Time Since New Symptoms Appeared	CT Myelography Diagnosis	Time from CT Myelography to MR	MR Diagnosis	IOSS and/or Surgical Findings
1	38	2 yr	Advancing paraplegia; sphincter dysfunction	Symptoms not new	—		SAC (T1–>conus)	SAC (T1–>conus)
2	25	5 yr	Increasing pain in upper chest; increasing spasticity of lower extremities	10 mo	IMC (T2–>T3)* & SAC (T4–>T5)	3 mo	SAC (T2–>T3) & SAC (T4–>T5)	IMC (T2–>T3) & SAC (T4–>T5)
3	21	14 yr	Low back pain; bladder-function changes	1 yr	—		SAC (T3–>T9)	SAC (T3–>T9)
4	No def. inj.	—	Bladder-function problems; pins & needles sensation in lower extremities; inability to lie in certain positions	6–7 mo	Small cord; prominent SAS posteriorly (most consistent with SAC) (mid to low thoracic cord)	1 mo	SAC (T4–>T7)	SAC (T4–>T7)
5	48	8 yr	Exacerbation of back pain; spasms	1 yr	—		SAC (C6–>T8) & IMC (T8–>conus)	SAC (C6–>T8) & IMC (T8–>conus)
6	22	4 mo	Continuation of collapse of anterior aspect of C6 despite placement in halo	Few mos.	Myelomalacia (C3–>C4)		—	SAC (C3–>C4) & myelomalacia (C2–>C7)
7	38	1 yr	Decerebrate posturing on extension of lower extremities; urinary incontinence; chronic constipation	Symptoms not new	IMC (C2–>C6 & mid thoracic) SAC (low cervical to mid thoracic)		—	IMC (C2–>C6 & mid thoracic) SAC (low cervical to mid thoracic)
8	30	7 mo	Intractable pain; progressive dysesthesias	Few mos.	SAC (T2–>T4)		—	SAC (T2–>T4)
9	19	8 yr	Pain in lower cervical region and between scapulae	1 mo	IMC (C4–>C7)		—	SAC and myelomalacia (mid–> low cervical spine)
10	25	15 yr	Deterioration in gait	1 yr	—		SAC (T9–>T11) & low intensities of cord just above T9	Myelomalacia (T6–>T9); SAC (T9–>T11); & IMC T11–>lumbar)
11	31	30 yr	Inability to walk; pain in left hip radiating to left lower extremity	7–8 mo	—		SAC (T10)	Pseudomeningocele (T10); SAC (T10); residual tumor (T10–>T11)
12	29	2 yr	Difficulty walking	1 yr	—		SAC (C7–>T10) & IMC (T10–>T11)	SAC (C7–>T10) & IMC (T8–>T11)
13	30	4 yr	Difficulty walking	Few mos.	Block at T10 level	4 days	SAC (C7–>T4)	Arachnoiditis
14	28	10 mo	Inability to walk	8 mo	—		SAC (T4–>T10)	Arachnoiditis
15	29	11 yr	Paraplegia; pain in waist	2 yr	—		SAC (T5–>T11)	Awaiting surgery

Note.—IOSS = intraoperative spinal sonography, SAC = subarachnoid cyst, SAS = subarachnoid space, IMC = intramedullary cyst.

* When referring to the extent of a lesion, C refers to the cervical spine followed by the number corresponding to the level. T refers to the thoracic spine. The superior extent is always on the left followed by an arrow, which is followed by the inferior extent.

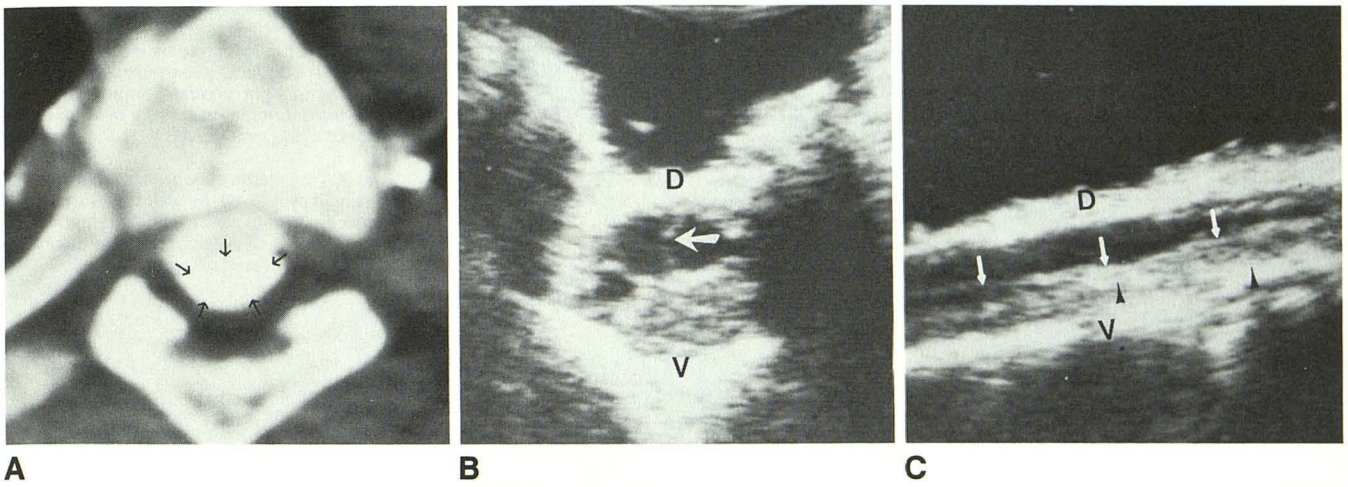

Fig. 1.—Case 8.

***A*, Delayed CT myelogram in patient with dorsal subarachnoid cyst (*arrows*) caused by gunshot wound to T5. Spinal cord is nearly isodense with surrounding cyst because metrizamide has penetrated into abnormal cord substance. The cord and cyst can be separated. This increased density of cord corresponds to area of increased echogenicity of cord in Figs. 1B and 1C (see text also).**

***B* and *C*, Transverse (*B*) and longitudinal (*C*) intraoperative spinal sonograms (D = dorsal, V = ventral). Subarachnoid cyst consists of a septated anechoic extramedullary collection (*arrow* in *B*) compressing the cord and displacing it anteriorly. Note abnormal echogenicity (*arrowheads* in *C*) of cord at level of maximum compression. Dorsal aspect of cord is outlined by *white arrows* in *C*. This cyst was shunted into distal subarachnoid space.**

with metrizamide, and three with both MR and CT myelography. Fourteen patients were operated on and were evaluated during surgery with intraoperative spinal sonography. Observers were not blinded to the surgical results or other preceding imaging studies when available. Pertinent data are summarized in Table 1.

MR images were obtained in the sagittal plane on a 0.5-T unit.* In the majority of cases, contiguous 5-mm-thick images were obtained using spin-echo pulse sequences of 1000/26/2 (TR/TE/excitations) for T1-weighted images and 2000/80/2 for T2-weighted images. Axial images supplemented the examination in the majority of cases. The images in seven of the cases were acquired and displayed on a 256 × 256 matrix. In the remaining four cases a 192 × 256 matrix was employed for data acquisition but displayed as 256 × 256. In four cases, motion-induced artifacts were suppressed by the application of extra gradient pulses termed MAST (motion artifact suppression technique) [7]. In one patient (case 12), a field echo (or gradient recalled echo) pulse sequence, 500/18/20° (TR/TE/flip angle), and a cardiac gated sequence (1924/80/2) were used.

With CT myelography, contiguous 5-mm axial sections were obtained as a delayed study 3–5 hr after routine metrizamide myelography. In one case a CT scan was obtained immediately after myelography and another, delayed, CT scan was obtained 3 hr later. The time interval between CT myelography and MR was 4 days, 1 month, and 3 months, respectively, in the three cases in which both studies were done.

Results

Table 1 summarizes the clinical and radiographic results in our patients. Six of the patients (cases 2, 3, 6, 7, 8, and 9) had sustained trauma. Three of these injured patients developed a SAC in the cervical area near the area of trauma and one of these cysts extended into the thoracic area. Three had thoracic SAC, also in proximity to the area of trauma. Six of the patients (cases 1, 10, 12, 13, 14, and 15) had undergone epidural anesthesia leading to arachnoiditis and subsequent SAC in the thoracic region. One patient (case 5) had undergone a traumatic lumbar puncture and developed a thoracic SAC. One patient (case 11) had surgery for a thoracic meningioma 30 years prior to this evaluation and developed a thoracic SAC. In one patient (case 4), a definite antecedent for a thoracic SAC could not be established, although the patient had been a football player and trauma was suspected as the underlying cause. The elapsed time from injury to the present evaluation ranged from 4 months to 30 years. Thirteen of the patients developed new symptoms, and the elapsed time from their first appearance to the present radiologic evaluation ranged from 1 month to 2 years.

Water-soluble contrast myelography followed by CT was performed in seven of the patients. In four of these, accurate interpretations were made. In these four cases, SAC was identified as an intradural extramedullary collection of contrast, sometimes of slightly higher density than the remainder of the subarachnoid space, which was producing some mass effect on the cord with indentation of the cord in two cases (Figs. 1 and 2). Adhesions or septations were never identified on CT myelograms, although these were frequently seen on sonograms (Fig. 1). In a review of the three cases in which a diagnosis was not established, we found that frequently the density of the SAC was not greater than the surrounding structures (Fig. 3). Concurrent myelomalacia also interfered with the diagnosis of a SAC as it became difficult to distinguish myelomalacic cord from SAC on the delayed studies (Figs. 3 and 4).

MR was performed in 11 patients. On T1-weighted images, a SAC was seen as a low-intensity signal collection that became higher in intensity on T2-weighted images (Fig. 5),

* Picker International, Highland Heights, OH.

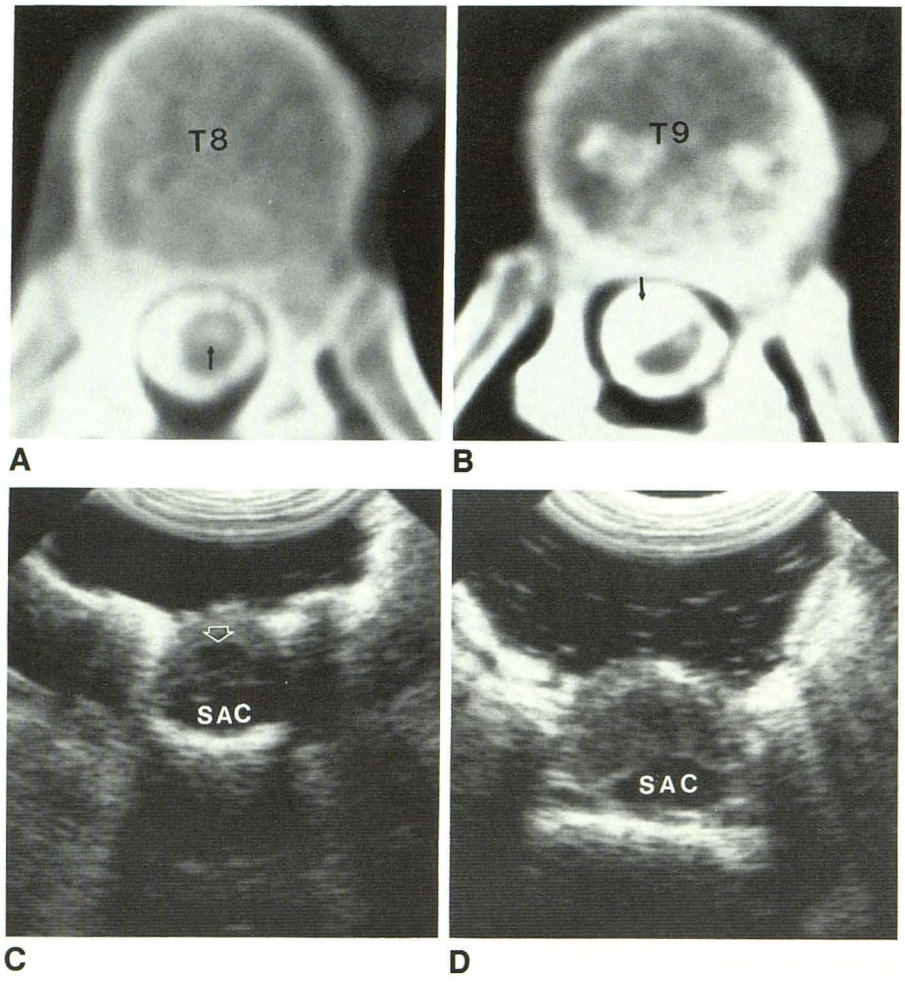

Fig. 2.—Case 7.

***A* and *B*, CT myelograms in patient with trauma to lower cervical spine subsequent to motor vehicle accident. Subarachnoid cyst (*arrow* in *B*) is in right ventral portion of canal, indenting the anterolateral surface of cord. Note central cord cyst (*arrow* in *A*). (*B* is 2 cm below *A*.)**

***C* and *D*, Transverse sonograms show ventral subarachnoid cyst (SAC) as well as central area of sonolucency consistent with intramedullary cyst (*arrow* in *C*). Cyst was surgically shunted into distal subarachnoid space.**

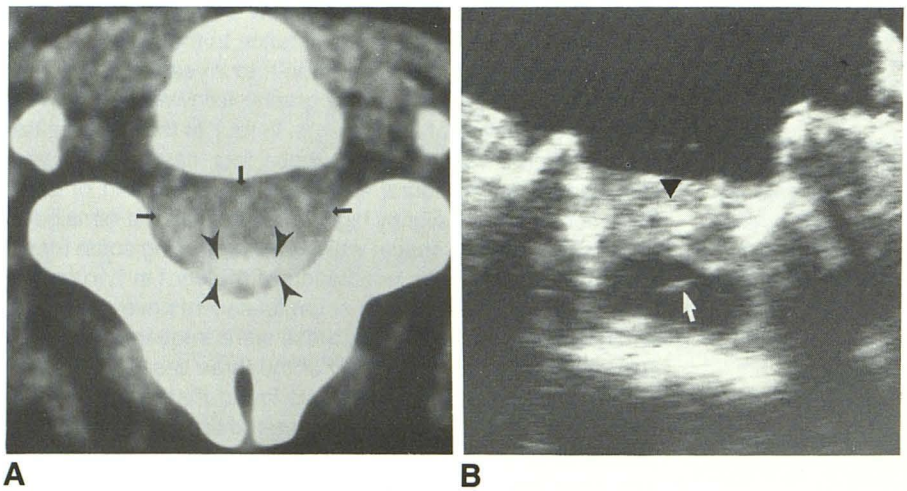

Fig. 3.—Case 6.

***A*, Delayed CT myelogram in patient with subluxation at C4–C5 level subsequent to auto accident. Abnormal density within cord was thought to represent myelomalacia. Dense contrast in posterior canal was thought to represent contrast layering in posterior subarachnoid space in supine position. No subarachnoid cyst was diagnosed; however, during surgery and intraoperative sonography (Fig. 3B), it was shown that the ventral collection of lower density represented a large subarachnoid cyst (*arrows*), indenting a myelomalacic cord posteriorly (*arrowheads*). The cyst in this case was of lesser density than the posteriorly located myelomalacic cord.**

***B*, Transverse sonogram shows septated ventral subarachnoid cyst (*arrow*), which was compressing cord and displacing it posteriorly. There is generalized increased echogenicity of the cord (*arrowhead*), typical of myelomalacia. The dense contrast in posterior subarachnoid space in *A* probably represents the myelomalacic cord, which was displaced dorsally by the cyst.**

paralleling CSF intensity. These collections usually produced mass effect on the cord with indentation of the cord (Figs. 6–8). Irregularities of the surface of the cord were also frequently present (Figs. 7 and 8). In addition, septations within the SAC were seen in approximately half the cases (e.g., Figs. 6 and 8). MR accurately diagnosed a SAC in all cases. In one patient (case 2), an additional intramedullary cyst at a slightly higher level was wrongly diagnosed as a SAC.

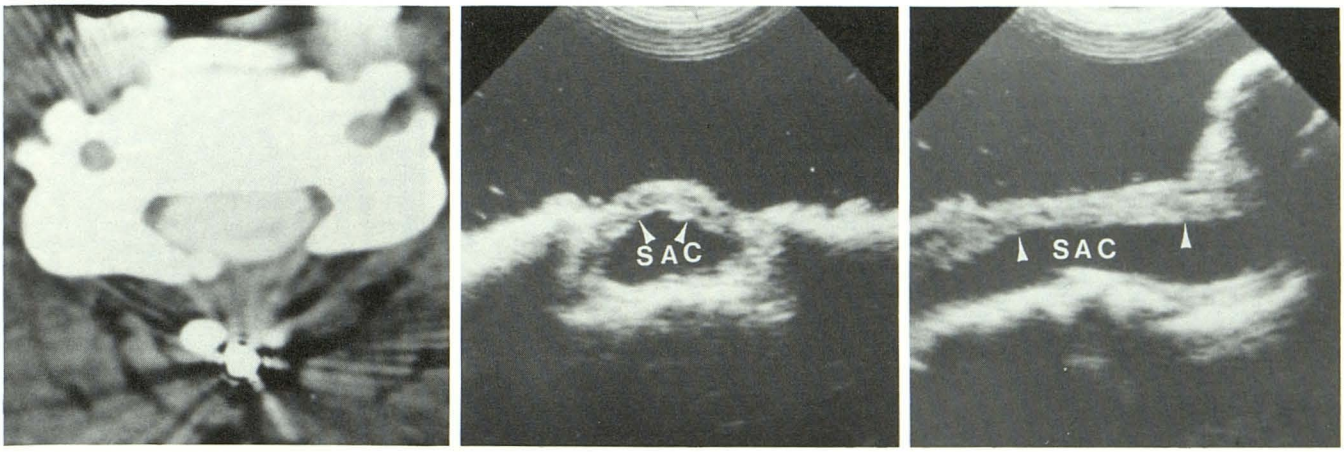

Fig. 4.—Case 9.
***A*, 4-hr-delayed CT myelogram of cervical spine in a patient with quadraplegia resulting from a diving accident 8 years prior to this evaluation. Nearly complete opacification of spinal contents was interpreted as either an intramedullary cyst or a diffuse myelomalacia.**
***B* and *C*, Sonograms show a ventral subarachnoid cyst (SAC) elevating and compressing undersurface of cord (*arrowheads*). The dura was opened and adhesions between pial surface of cord and dura were lysed. A shunt catheter was then directed into the ventral SAC at C6–C7 level.**

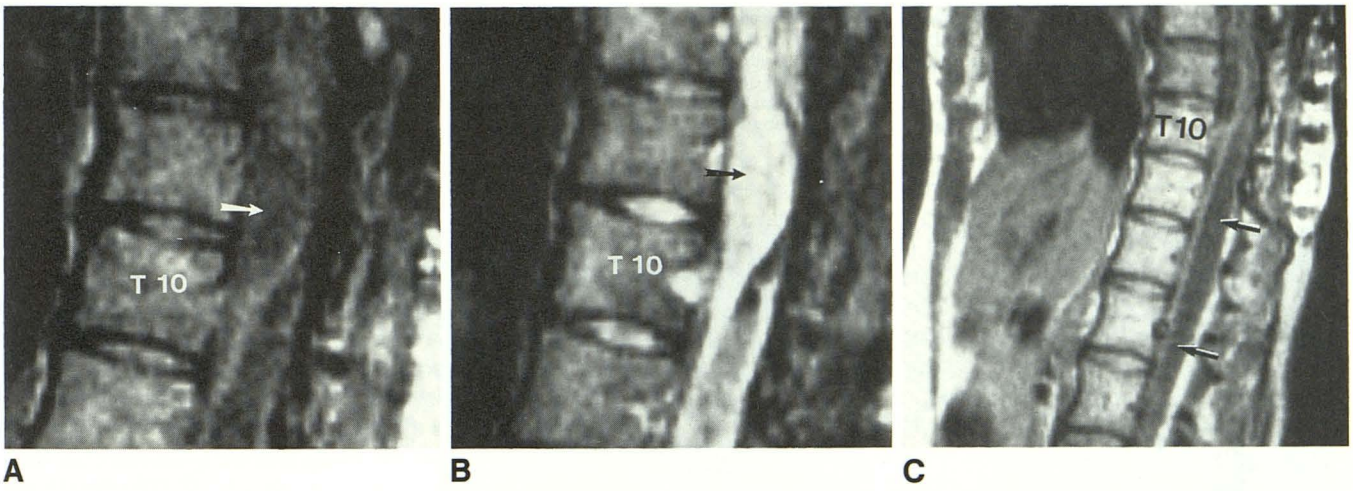

Fig. 5.—Case 10: Patient with arachnoiditis subsequent to receiving epidural anesthesia for childbirth.
***A* and *B*, T1-weighted MR images (1000/26) show focal area of low-intensity signal that becomes hyperintense on T2-weighted images (2000/80), representing a subarachnoid cyst (*arrows*) at T9 and T10.**
***C*, Note intramedullary cyst in low thoracic cord (*arrows*) below the level of the subarachnoid cyst.**

In one case, additional pulse sequences were obtained in an attempt to understand the pathophysiological mechanisms involved in the propagation of these cysts (Fig. 9). The T2 sequence without MAST (Fig. 9A) showed that there was significant spin dephasing of fluid within the SAC because of motion. In the MAST sequence there was no difference in the intensity signal within the SAC and that of the CSF outside the SAC. This suggested that the SAC had flow that was comparable to the remaining CSF. Cardiac gated images in this case were also effective in diminishing flow artifacts caused by presumed cyst-fluid pulsations. When the cyst fluid was hyperintense relative to CSF on nongated, non-MAST studies, we suggested that the cyst fluid was loculated and unable to undergo enough motion to cause spin dephasing (Fig. 5).

Since the majority of patients (12/15) had only MR or CT myelography, a limited comparison of these two techniques in the same patient was done (i.e., three direct comparisons). A second study in these 12 patients was thought to be clinically unwarranted. Nonetheless, the relative efficacy of the two techniques could be determined in all 15 patients.

Turning to the three cases in which both techniques—MR and CT myelography—were performed, SAC was correctly diagnosed by both methods in cases 2 and 4. In case 13, a SAC in the upper thoracic spine was correctly diagnosed on MR but missed on CT myelography. The block to the flow of contrast medium in this case did not allow contrast to enter the SAC for a correct interpretation.

Intraoperative spinal sonography was performed in 12 patients in this study. In all these patients the SAC was seen as

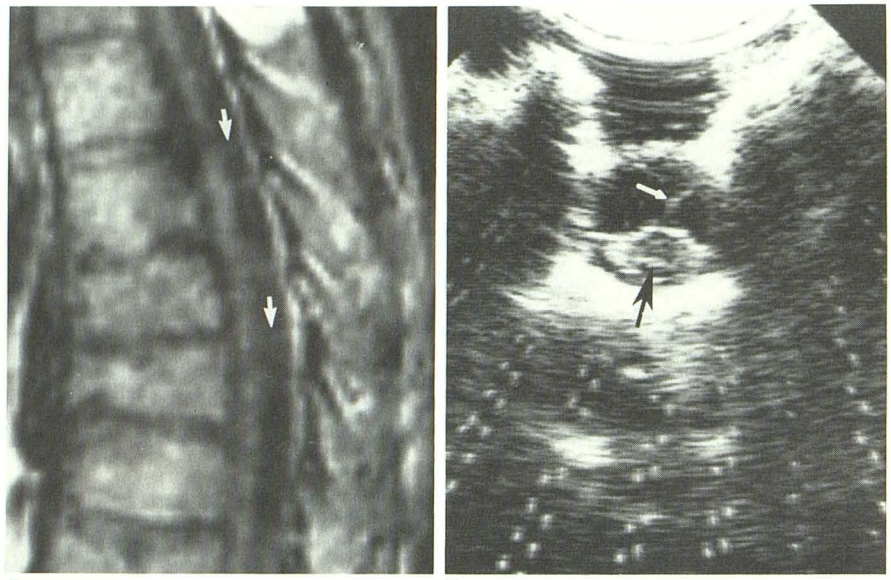

Fig. 6.—Case 3.

A, T1-weighted MR images (1000/26) in patient with dorsal subarachnoid cyst, which is producing a mass effect on posterior surface of cord. There are thin septations in cyst separating it into discrete compartments (*arrows*).

B, Transverse sonogram confirms septations (*white arrow*) within subarachnoid cyst. There is normal echogenicity (low-level echoes) of the cord and retention of the central echo (*black arrow*). Compare this with the abnormal-appearing cord in Figs. 1B, 1C, and 3B. This patient had a T3 through T9 laminectomy. The dorsal subarachnoid cyst walls were fenestrated and the cyst drained.

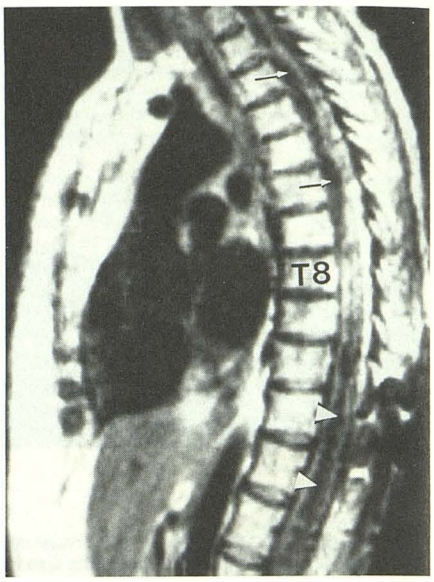

Fig. 7.—Case 5. T1-weighted MR image (1000/26) shows irregular cord surface and ventral subarachnoid cyst that is producing a mass effect on anterior surface of cord from C6 to T8 (*arrows*). Note also the associated spinal cord cyst (*arrowheads*) extending from T8 to conus showing the "stacked coin" appearance. An intramedullary shunt placed 3 years previously was revised, and a shunt was placed into the subarachnoid cyst.

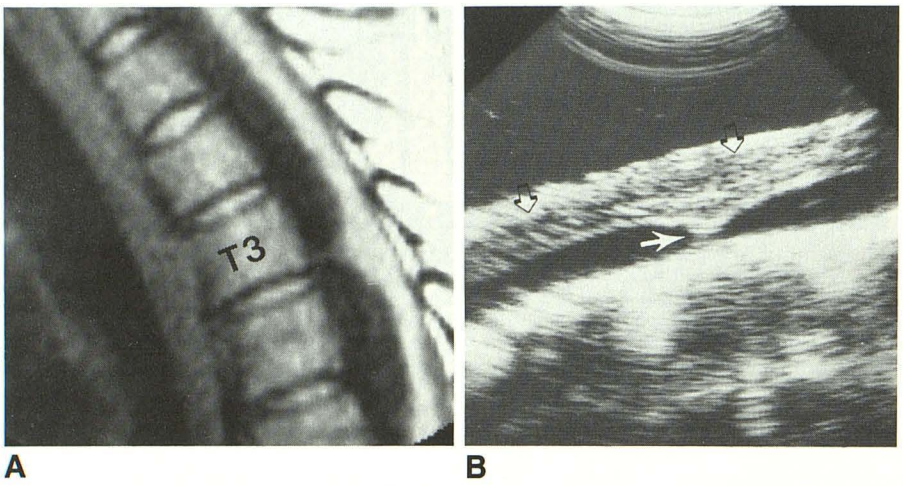

Fig. 8.—Case 1: This patient was given local epidural anesthesia for surgery on a herniated disk.

A, T1-weighted MR image (1000/26) shows irregular cord surface, CSF collection ventral to the low cervical cord, and septation within subarachnoid cyst.

B, The abnormalities seen in *A* are appreciated on this sonogram; specifically, the cord (*open arrows*), tethered dorsally to the posterior dura, the subarachnoid cyst, and the intracyst septation (*closed arrow*). After laminectomy from T7 to T12, the cord was untethered.

an anechoic extramedullary collection that displaced the cord. Frequently, this anechoic area had fibrous septations (Figs. 1B, 3B, 6B, and 8B) and was associated with other abnormalities of the cord, such as intramedullary cysts, at the same or other levels (Fig. 2C).

Associated abnormalities were seen in seven of the 15 cases. These included myelomalacia and spinal cord cyst (Table 1). These abnormalities were found to be present at a site distant from the level of the SAC more than half the time (Figs. 5 and 7).

Discussion

Inflammation resulting from infection, trauma, surgery, or blood or contrast medium in the CSF has been suggested as the causative agent in the formation of a SAC [2, 8–11]. These cysts arise because granulation tissue forms within the subarachnoid space and fluid may collect in irregular compartments. In addition, chronic spinal arachnoiditis frequently leads to fibrosis of the arachnoid and this may cause progressive dysfunction of the spinal cord [2]. It has also been

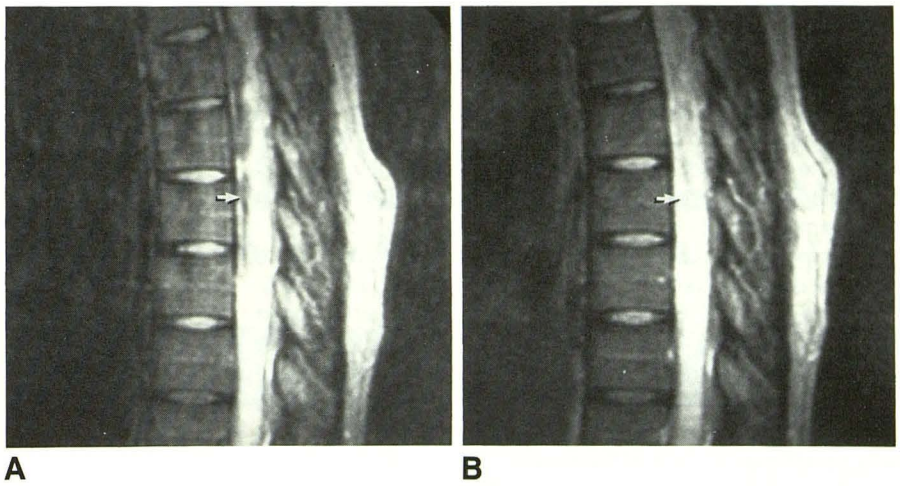

Fig. 9.—Case 12.
***A*, T2-weighted MR image (2000/80) in a patient with arachnoiditis and a ventral subarachnoid cyst that is producing a mass effect on the cord (*arrow*).**
***B*, T2-weighted MR image (2000/80) with extra gradient pulses (see text) to compensate for flow effects (MAST sequence). Note that cyst, which had been hypointense in *B*, becomes more hyperintense (*arrow*). This suggests that subarachnoid cyst had flow comparable to remaining CSF.**

suggested that inflammation may cause constricting bands to develop in the arachnoid, resulting in arachnoid or subarachnoid cysts that behave as space-occupying lesions [12].

SAC may cause neurologic symptoms by compressing the spinal cord or nerve roots [13]. Pain may be episodic in character, which suggests variation in the size of these cysts, probably due to movement of CSF through a small opening, a "ball valve" mechanism that intermittently obstructs the cyst [2]. There may be postural accentuation of pain as the cysts enlarge with different positions and cause increasing compression on neural structures [13]. In a series of nine intradural SACs, Kendall et al. [13] found paresis, usually with a sensory level in all cases. Many of the patients had local pain with and without evidence of bony erosion on plain films.

In our cases, once compression of neural structures was appreciated on MR or water-soluble myelography followed by CT, surgery was performed. The cysts were excised, fenestrated, or shunted depending on the size of the cysts and how well they were encapsulated. Although our investigation was not directed at the efficacy of treatment, it has been our experience that the posttraumatic cysts responded best to surgery. Those patients with cysts resulting from inflammation caused by epidural anesthesia did well immediately after surgery but deteriorated in the long-term follow-up. This may be due to intrinsic damage to the cord that was vascular in nature.

Our experience suggests that in studying these cysts, MR is more accurate than water-soluble myelography or CT. CT myelography was able to accurately diagnose SAC in four of seven cases. MR accurately diagnosed SAC in all 10 cases that were also surgically proved. A CSF-containing lesion can be diagnosed on MR by the presence of long T1 and long T2 relaxation times. The finding that indicates that such a lesion is located in the subarachnoid space is the presence of mass effect on the cord, with identation and irregularities of the cord surface (Figs. 7 and 8A). An extradural lesion would not produce irregularities of the cord surface and would not widen the corresponding subarachnoid space. Intracystic septations were also frequently identified on sonography and MR. These reflect the healing of an inflammatory process or traumatic event similar to those seen within intramedullary cysts [14]. Concerning the pathophysiological mechanism involved in the function and propagation of acquired SAC, it appears that these cysts behave in a variable fashion. In some instances (Fig. 5), the SAC may be loculated and not in direct communication with the subarachnoid space. The result is a nonpulsatile and nonturbulent fluid collection manifested by a lack of dephasing on T2 images (Fig. 5B). In other cases (Fig. 9) the cysts most likely communicated freely with the rest of the subarachnoid space because the cysts showed relative hypointensity on routine T2 images (Fig. 9A), indicative of CSF motion. We postulate that the variation in signal intensity between subarachnoid cysts is due to the degree of scarring and septation of the cysts, which in turn causes CSF flow variation.

It occasionally may be difficult on MR to distinguish intramedullary from extramedullary cysts. In this regard, the presence of a "stack of coins" appearance would be helpful as it indicates the presence of a cyst within the cord (Fig. 7). Another possible pitfall with MR that we have encountered is the presence of a large subarachnoid space associated with a small atrophic cord that is attached to either the ventral or dorsal dura, in which case the enlarged subarachnoid space may be confused with a SAC with compression of the cord. This problem, however, would also be encountered with other imaging methods.

A SAC may be difficult to differentiate from myelomalacia on CT myelography when both are present simultaneously, since on delayed studies both would be expected to show an area of increased density (Fig. 4). In this regard, a finding that may be helpful, if present, is the fact that a SAC may be of a different density than the surrounding subarachnoid space and may also be of a different density from myelomalacic cord. In case 6 (Fig. 3A), the SAC was of lower density than the myelomalacic cord. This is in contradiction to the literature, where it has been stated that a SAC might be expected to be denser than the surrounding subarachnoid space on de-

layed CT myelography because of a lack of free diffusion into and out of the cyst [3, 13]. Instead, it seems that a SAC may be of increased or decreased density depending on the mechanisms of CSF flow in and out of these cysts and the position of the patient at the time of the myelogram and CT examination. The cyst and its neck are most frequently situated posterior to the spinal cord, so that entry of contrast medium occurs more readily in the supine position [5, 13].

An important aspect of the surgical management of these patients is the presence of associated spinal cord abnormalities, including myelomalacia and spinal cord cysts. These findings occurred with equal frequency at and away from the level of injury. Therefore, when a SAC is found, other such lesions are not unexpected. Since MR can image a long segment of cord noninvasively, it is particularly suited for the preoperative evaluation of the patient [15].

In the workup of patients with a SAC, we suggest the following protocol: sagittal T1- and T2-weighted spin-echo pulse sequences without the use of cardiac gating or extra gradients to suppress motion should be obtained through the area of interest. Then a sagittal T1-weighted spin-echo pulse sequence should be obtained to include a larger field of interest for associated lesions, which, if detected, should be fully evaluated. Recent work [16] has indicated that cardiac gated cine MR may be helpful in determining pulsatility of the SAC.

In summary, our results indicate that in patients who have had prior spinal injury or spinal inflammatory changes, and who have progressive neurologic symptoms, MR is the only preoperative study needed to determine the presence of a SAC and of associated lesions. A CSF-containing SAC will be hypointense on T1-weighted images and will have variable intensity on routine T2-weighted images depending on the movement of CSF within the cyst. SAC will frequently produce extrinsic mass effect on the cord. And because associated intramedullary lesions are commonly present, evaluation should include a complete survey of the spinal cord, since these associated lesions may be found away from, and at the level of, injury.

REFERENCES

1. Swany KS, Reddy AK, Srivastava VK, Das BS, Reddy GN. Intraspinal arachnoid cyst. *Clin Neurol Neurosurg* **1984**;86:145–148
2. Duncan AW, Hoare RD. Spinal arachnoid cysts in children. *Radiology* **1978**;126:423–429
3. Post MJD, Green BA. The use of computed tomography in spinal trauma. *Radiol Clin North Am* **1983**;21:327–375
4. Perret G, Green DJ. Diagnosis and treatment of intradural arachnoid cysts of the thoracic spine. *Radiology* **1962**;79:425–429
5. Gado M, Hodges F, Petit J. Computed tomography of the spine with metrizamide. In: Post MJD, ed. *Computed tomography of the spine*. Baltimore: Williams & Wilkins, **1984**
6. Odin M, Runstrom G. Iodized oils as an aid to diagnosis of lesions of the spinal cord and a contribution to the knowledge of adhesive circumscribed meningitis. *Acta Radiol* **1928**;(Suppl. 7):3–85
7. Pattany PM, Phillips JJ, Chiu LC, et al. Motion artifact suppression technique (MAST) for MR imaging. *J Comput Assist Tomogr* **1987**;11:369–377
8. Benini A. Chronic circumscribed adhesive and cystic spinal leptomeningitis. Report of four cases, with special references to microsurgical treatment. *Surg Neurol* **1973**;1:223–228
9. Davidoff LM, Gass H, Grossman J. Post-operative spinal adhesive arachnoiditis and recurrent spinal cord tumor. *J Neurosurg* **1947**;4:451–464
10. MacKay RP. Chronic adhesive spinal arachnoiditis: a clinical and pathologic study. *JAMA* **1939**;112:802–808
11. McLaurin RL, Bailey OT, Schurr PM, et al. Myelomalacia and multiple cavities of spinal cord secondary to adhesive arachnoiditis: an experimental study. *Arch Pathol* **1954**;57:138–146
12. Trevor-Hughes J. *Pathology of the spinal cord*. London: Lloyd-Luke, **1966**:133–135
13. Kendall BE, Valentine AR, Keis B. Spinal arachnoid cysts: clinical and radiological correlation with prognosis. *Neuroradiology* **1982**;22:225–234
14. Quencer RM. The injured spinal cord: evaluation with magnetic resonance and intraoperative sonography. *Radiol Clin North Am* **1988**;26:1025–1045
15. Quencer RM, Sheldon JJ, Post MJD, et al. Magnetic resonance imaging of the chronically injured cervical spinal cord. *AJNR* **1986**;7:457–464, *AJR* **1986**;147:125–132
16. Post MJD, Quencer RM, Green BA, Hins RS, Horen M, Labus J. The role of cine-MR in the evaluation of the pulsatile characteristics of posttraumatic spinal and subarachnoid cord cysts (abstr). *AJNR* **1988**;9:1001–1002